

A Variational Asymptotic Micromechanics Model for Predicting Conductivity of Composite Materials

Tian Tang and Wenbin Yu¹

*Department of Mechanical and Aerospace Engineering
Utah State University, Logan, Utah 84322-4130, USA*

Abstract

The focus of this paper is to extend the variational asymptotic method for unit cell homogenization (VAMUCH) to predict the effective thermal conductivity and local distribution of temperature field of heterogeneous materials. Starting from a variational statement of the conduction problem of the heterogeneous continuum, we formulate the micromechanics model as a constrained minimization problem using the variational asymptotic method. To handle realistic microstructures in applications, we implement this new model using the finite element method. For validation, a few examples are used to demonstrate the application and accuracy of this theory and companion code. Since heat conduction is [mathematically](#) analogous to electrostatics, magnetostatics, and diffusion, the present model can also be used to predict effective [dielectric](#), [magnetic](#), and diffusion properties of heterogeneous materials.

Key words: Homogenization; Heterogeneous; Conductivity; Variational Asymptotic Method; Micromechanics

1 Introduction

Along with increased knowledge and manufacturing techniques for materials, more and more materials are made with engineered microstructures to achieve better performance. To successfully design and fabricate these materials, we need efficient high-fidelity analysis tools to predict their effective properties. Many composites are applied in temperature sensitive environments such as

¹ Corresponding author: +1-435-7978246 (tel.); +1-435-7972417 (fax)
Email address: wenbin.yu@usu.edu (Wenbin Yu).

electronic packaging and thermal protection systems. Accurate prediction of thermal properties such as the specific heat, coefficients of thermal expansion, and thermal conductivity becomes important for such applications. In this paper, we focus on developing a model to predict effective thermal conductivity and associated local temperature and heat flux distribution within the heterogeneous materials.

The effective thermal conductivity of composites [is](#) strongly affected by many parameters including the properties, volume fractions, distributions, and orientations of constituents. Numerous models have been proposed to predict the effective thermal conductivity (Progelhof et al., 1976). [These models](#) include simple rules of [mixtures](#), self consistent scheme (Hashin, 1968), generalized self consistent scheme (Lee et al., 2006), finite element method (Islam and Pramila, 1999; Ramani and Vaidyanathan, 1995; Xu and Yagi, 2004; Kumlutas and Tavman, 2006), effective unit cell approach (Ganapathy et al., 2005) and variational bounds (Hashin and Shtrikman, 1962). Very recently, a new framework for micromechanics modeling, namely variational asymptotic method for unit cell homogenization (VAMUCH) (Yu and Tang, 2007a), has been introduced using two essential assumptions [in the context of](#) micromechanics for composites with an identifiable unit cell (UC):

- **Assumption 1** The exact field variable has volume average over the UC. For example, if ϕ is the exact temperature within the UC, there exist ψ such that

$$\psi = \frac{1}{\Omega} \int_{\Omega} \phi \, d\Omega \equiv \langle \phi \rangle \quad (1)$$

where Ω denotes the domain occupied by the UC and its volume, [and symbol \$\equiv\$ denotes a definition.](#)

- **Assumption 2** The effective material properties obtained from the micromechanical analysis of the UC are independent of the geometry, the boundary conditions, and loading conditions of the macroscopic structure, which means that effective properties are assumed to be the intrinsic properties of the material when viewed macroscopically.

[Note that](#) these assumptions are not restrictive. The mathematical meaning of the first assumption is that the exact solutions of the field are integrable over the domain of UC, which is true almost all the time. The second assumption implies that we will neglect the size effects of the material properties in the macroscopic analysis, which is an assumption often made in the conventional continuum mechanics. Of course, the micromechanical analysis of the UC is only needed and appropriate if $\eta = h/l \ll 1$, with h as the characteristic size of the UC and l as [the macroscopic size](#) of the macroscopic material.

This new micromechanical modeling approach has been successfully applied to predict [thermo-mechanical](#) properties including elastic properties, coefficients of thermal expansion, and specific heats (Yu and Tang, 2007a,b). In this work,

we will use this approach to construct micromechanics models for effective thermal conductivity and the corresponding local fields such as temperature and heat flux within UC.

2 Theoretical Formulation

VAMUCH formulation uses three coordinate systems: two Cartesian coordinates $\mathbf{x} = (x_1, x_2, x_3)$ and $\mathbf{y} = (y_1, y_2, y_3)$, and an integer-valued coordinate $\mathbf{n} = (n_1, n_2, n_3)$ (see Fig. 1). We use x_i as the global coordinates to describe the macroscopic structure and y_i parallel to x_i as the local coordinates to describe the UC (Here and throughout the paper, Latin indices assume 1, 2, and 3 and repeated indices are summed over their range except where explicitly indicated). We choose the origin of the local coordinates y_i to be the geometric center of UC. For example, if the UC is a cube with edge lengths d_i , then $y_i \in [-\frac{d_i}{2}, \frac{d_i}{2}]$. To uniquely locate a UC in the heterogeneous material we also introduce integer coordinates n_i . The integer coordinates are related to the global coordinates in such a way that $n_i = x_i/d_i$ (no summation over i). It is emphasized although only square array is sketched in Fig. 1, the present theory has not such limitations.

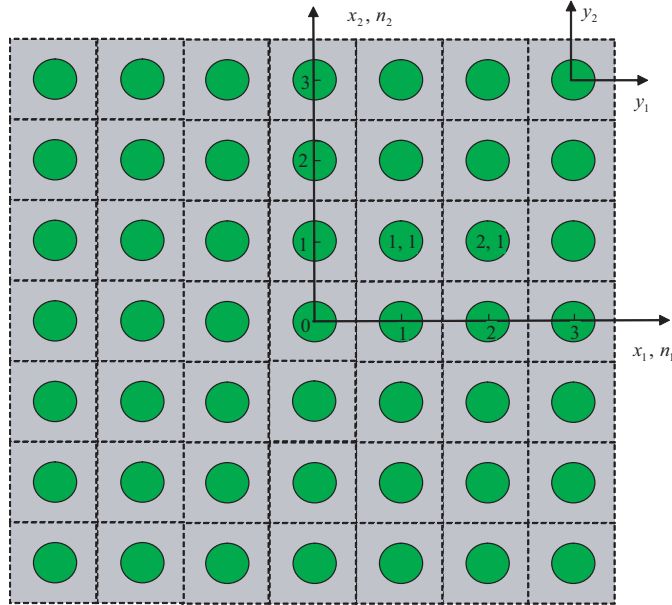


Fig. 1. Coordinate systems for heterogeneous materials (only two-dimensional (2D) square array UC is drawn for clarity)

As implied by Assumption 2, we can obtain the same effective properties from an imaginary, unbounded, and unloaded heterogeneous material with the same microstructure as the real, loaded, and bounded one. Hence we could derive the

micromechanics model from an imaginary, unloaded, heterogeneous material which completely occupies the three-dimensional (3D) space \mathcal{R} and composes of infinitely many repeating UCs. The solution of steady-state conduction problem, which is sufficient for us to find the effective thermal conductivity, can be obtained by the stationary value problem of the summation of “energy” integral of all the UCs (Hashin, 1968; Berdichevsky, 1977), which is:

$$\Pi = \sum_{n=-\infty}^{\infty} \frac{1}{2} \int_{\Omega} K_{ij} \phi_{,i} \phi_{,j} d\Omega \quad (2)$$

where K_{ij} are components of the second-order thermal conductivity tensor, and

$$\phi_{,i}(\mathbf{n}; \mathbf{y}) = \frac{\partial \phi(\mathbf{n}; \mathbf{y})}{\partial y_i} \quad (3)$$

with $(\cdot)_{,i} \equiv \frac{\partial(\cdot)}{\partial y_i}$. Here ϕ is a function of the integer coordinates and the local coordinates for each UC. In view of the fact that the infinite many UCs form a continuous heterogeneous material, we need to enforce the continuity of the temperature field ϕ on the interface between adjacent UCs, which is (n_1, n_2, n_3) :

$$\begin{aligned} \phi(n_1, n_2, n_3; d_1/2, y_2, y_3) &= \phi(n_1 + 1, n_2, n_3; -d_1/2, y_2, y_3) \\ \phi(n_1, n_2, n_3; y_1, d_2/2, y_3) &= \phi(n_1, n_2 + 1, n_3; y_1, -d_2/2, y_3) \\ \phi(n_1, n_2, n_3; y_1, y_2, d_3/2) &= \phi(n_1, n_2, n_3 + 1; y_1, y_2, -d_3/2) \end{aligned} \quad (4)$$

The exact solution of steady heat conduction problem will minimize the summation of “energy” integral in Eq. (2) under the constraints in Eqs. (1), (4). To avoid the difficulty associated with discrete integer arguments, we can reformulate the problem, including Eqs. (2), (3), and (4), in terms of continuous functions using the idea of quasicontinuum (Kunin, 1982). The corresponding formulas are listed below.

$$\Pi = \frac{1}{2} \int_{\mathcal{R}} \langle K_{ij} \phi_{,i} \phi_{,j} \rangle d\mathcal{R} \quad (5)$$

$$\phi_{,i}(\mathbf{x}; \mathbf{y}) = \frac{\partial \phi(\mathbf{x}; \mathbf{y})}{\partial y_i} \quad (6)$$

and

$$\begin{aligned} \phi(x_1, x_2, x_3; d_1/2, y_2, y_3) &= \phi(x_1 + d_1, x_2, x_3; -d_1/2, y_2, y_3) \\ \phi(x_1, x_2, x_3; y_1, d_2/2, y_3) &= \phi(x_1, x_2 + d_2, x_3; y_1, -d_2/2, y_3) \\ \phi(x_1, x_2, x_3; y_1, y_2, d_3/2) &= \phi(x_1, x_2, x_3 + d_3; y_1, y_2, -d_3/2) \end{aligned} \quad (7)$$

Using the technique of Lagrange multipliers, we can pose the thermal conduc-

tion problem as a stationary value problem of the following functional:

$$\begin{aligned}
J = & \int_{\mathcal{R}} \left\{ \left\langle \frac{1}{2} K_{ij} \phi_{,i} \phi_{,j} \right\rangle + \lambda (\langle \phi \rangle - \psi) \right. \\
& + \int_{S_1} \gamma_1 [\phi(x_1, x_2, x_3; d_1/2, y_2, y_3) - \phi(x_1 + d_1, x_2, x_3; -d_1/2, y_2, y_3)] dS_1 \\
& + \int_{S_2} \gamma_2 [\phi(x_1, x_2, x_3; y_1, d_2/2, y_3) - \phi(x_1, x_2 + d_2, x_3; y_1, -d_2/2, y_3)] dS_2 \\
& \left. + \int_{S_3} \gamma_3 [\phi(x_1, x_2, x_3; y_1, y_2, d_3/2) - \phi(x_1, x_2, x_3 + d_3; y_1, y_2, -d_3/2)] dS_3 \right\} d\mathcal{R}
\end{aligned} \tag{8}$$

where λ and γ_i are Lagrange multipliers [introduced to enforce the constraints in Eqs. \(1\) and \(7\)](#), respectively, and S_i are the surfaces with $n_i = 1$. The main objective of micromechanics is to find the real temperature field ϕ in terms of ψ , which is a very difficult problem because we have to solve this stationary problem for each point in the global system x_i as in Eq. (8). It will be desirable if we can formulate the variational statement posed over a single UC only. In view of Eq. (1), it is natural to express the exact solution ϕ as a sum of the volume average ψ plus the difference, such that

$$\phi(\mathbf{x}; \mathbf{y}) = \psi(\mathbf{x}) + w(\mathbf{x}; \mathbf{y}) \tag{9}$$

where $\langle w \rangle = 0$ according to Eq. (1). The very reason that the heterogenous material can be homogenized leads us to believe that w should be asymptotically smaller than ψ , *i.e.*, $w \sim \eta \psi$. Substituting Eq. (9) into Eq. (8) and making use of Eq. (6), we can obtain the leading terms of the functional according to the variational asymptotic method (Berdichevsky, 1977) as:

$$\begin{aligned}
J_1 = & \int_{\mathcal{R}} \left\{ \left\langle \frac{1}{2} K_{ij} w_{,i} w_{,j} \right\rangle + \lambda \langle w \rangle \right. \\
& + \int_{S_1} \gamma_1 [w(\mathbf{x}; d_1/2, y_2, y_3) - w(\mathbf{x}; -d_1/2, y_2, y_3) - \psi_{;1} d_1] dS_1 \\
& + \int_{S_2} \gamma_2 [w(\mathbf{x}; y_1, d_2/2, y_3) - w(\mathbf{x}; y_1, -d_2/2, y_3) - \psi_{;2} d_2] dS_2 \\
& \left. + \int_{S_3} \gamma_3 [w(\mathbf{x}; y_1, y_2, d_3/2) - w(\mathbf{x}; y_1, y_2, -d_3/2) - \psi_{;3} d_3] dS_3 \right\} d\mathcal{R}
\end{aligned} \tag{10}$$

where $(\cdot)_{;i} \equiv \frac{\partial(\cdot)}{\partial x_i}$. Although it is possible to carry out the variation of J_1 and find the Euler-Lagrange equations and associated boundary conditions for w , which results in inhomogeneous boundary conditions, [it is more convenient to use change of variables to reformulate the same problem so that the boundary conditions are homogeneous](#). Considering the last three terms in Eq. (10), we use the following change of variables to express w as:

$$w(\mathbf{x}; \mathbf{y}) = y_i \psi_{;i} + \zeta(\mathbf{x}; \mathbf{y}) \tag{11}$$

with ζ normally termed as fluctuation functions. We are free to choose the origin of the local coordinate system to be the center of UC, which implies the following constraints on ζ :

$$\langle \zeta \rangle = 0 \quad (12)$$

Substituting Eq. (11) into Eq. (10), we obtain a stationary value problem defined over UC for ζ , such that

$$\begin{aligned} J_\Omega &= \frac{1}{2} \langle K_{ij} (\psi_{;i} + \zeta_{,i}) (\psi_{;j} + \zeta_{,j}) \rangle + \lambda \langle \zeta \rangle \\ &+ \int_{S_1} \gamma_1 (\zeta^{+1} - \zeta^{-1}) dS_1 + \int_{S_2} \gamma_2 (\zeta^{+2} - \zeta^{-2}) dS_2 \\ &+ \int_{S_3} \gamma_3 (\zeta^{+3} - \zeta^{-3}) dS_3 \end{aligned} \quad (13)$$

with

$$\zeta^{+i} = \zeta|_{y_i=d_i/2} \quad \zeta^{-i} = \zeta|_{y_i=-d_i/2} \quad \text{for } i = 1, 2, 3 \quad (14)$$

where $\psi_{;i}$ will be shown later to be the components of the global temperature gradient vector for the effective material with homogenized material properties. The functional J_Ω in Eq. (13) forms the backbone of the present theory. This stationary problem can be solved analytically for very simple cases such as binary composites, however, for general cases we need to use numerical techniques such as the finite element method (FEM) to seek numerical solutions.

3 An Illustrative Example

To illustrate the solution procedure of the stationary problem of the functional in Eq. (13), we will consider a periodic binary composite made of anisotropic layers and the material axes are the same as the global coordinate x_i so that the material is uniform in the $x_1 - x_2$ plane and periodic along x_3 direction. A typical UC can be identified as shown in Fig. 2, with the dimension along y_3 as h and dimensions along y_1 and y_2 arbitrary. Let ϕ_1 and ϕ_2 denote the volume fraction of the first layer and the second layer, respectively, and we have $\phi_1 + \phi_2 = 1$.

Because of the uniformity of the structure in the $x_1 - x_2$ plane, we know that the solution of ζ will be independent of y_1 and y_2 , and is a function of y_3 only. Taking advantage of the this fact, we can specialize the functional in Eq. (13)

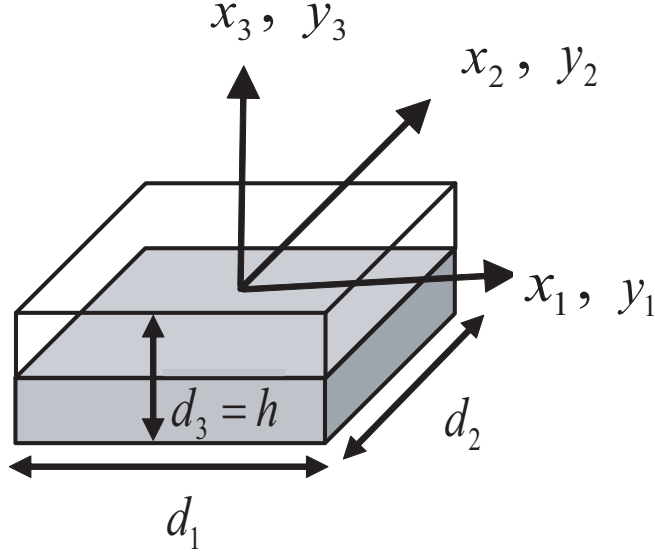


Fig. 2. Sketch of a binary composite

for this particular case in a matrix form as:

$$\begin{aligned}
J_{\Omega}^* = & \int_{S_3} \left\{ \int_{-\frac{h}{2}}^{(\phi_1 - \frac{1}{2})h} \left[\frac{1}{2} \Psi^{(1)T} K^{(1)} \Psi^{(1)} + \lambda \zeta^{(1)} \right] dy_3 \right. \\
& + \int_{(\phi_1 - \frac{1}{2})h}^{\frac{h}{2}} \left[\frac{1}{2} \Psi^{(2)T} K^{(2)} \Psi^{(2)} + \lambda \zeta^{(2)} \right] dy_3 \\
& \left. + \gamma_3 \left[\zeta^{(2)} \left(\frac{h}{2} \right) - \zeta^{(1)} \left(-\frac{h}{2} \right) \right] \right\} dS
\end{aligned} \tag{15}$$

with $\Psi^{(\alpha)} = [\psi_{;1} \ \psi_{;2} \ \psi_{;3} + \zeta_3^{(\alpha)}]^T$ for $\alpha = 1, 2$, and $\zeta^{(\alpha)}$ as the fluctuation functions of the temperature for each layer. The thermal conductivity matrix $K^{(\alpha)}$ is a fully populated symmetric matrix for a general anisotropic material, such that

$$K^{(\alpha)} = \begin{bmatrix} K_{11}^{(\alpha)} & K_{12}^{(\alpha)} & K_{13}^{(\alpha)} \\ K_{12}^{(\alpha)} & K_{22}^{(\alpha)} & K_{23}^{(\alpha)} \\ K_{13}^{(\alpha)} & K_{23}^{(\alpha)} & K_{33}^{(\alpha)} \end{bmatrix} \tag{16}$$

The corresponding differential statement of the variational statement in Eq. (15) can be obtained following normal procedures of the calculus of variations, as follows:

$$K_{33}^{(\alpha)} \zeta_{,33}^{(\alpha)} = \lambda \tag{17}$$

$$\int_{-\frac{h}{2}}^{(\phi_1 - \frac{1}{2})h} \zeta^{(1)} dy_3 + \int_{(\frac{1}{2} - \phi_2)h}^{\frac{h}{2}} \zeta^{(2)} dy_3 = 0 \tag{18}$$

$$\zeta^{(1)}\left(-\frac{h}{2}\right) = \zeta^{(2)}\left(\frac{h}{2}\right) \quad (19)$$

$$\zeta^{(1)}(\phi_1 h - h/2) = \zeta^{(2)}(\phi_1 h - h/2) \quad (20)$$

$$\begin{aligned} & K_{13}^{(1)} \psi_{;1} + K_{23}^{(1)} \psi_{;2} + K_{33}^{(1)} \left[\psi_{;3} + \zeta_{,3}^{(1)} \right] \Big|_{y_3 = -\frac{h}{2}} \\ &= K_{13}^{(2)} \psi_{;1} + K_{23}^{(2)} \psi_{;2} + K_{33}^{(2)} \left[\psi_{;3} + \zeta_{,3}^{(2)} \right] \Big|_{y_3 = \frac{h}{2}} \end{aligned} \quad (21)$$

$$\begin{aligned} & K_{13}^{(1)} \psi_{;1} + K_{23}^{(1)} \psi_{;2} + K_{33}^{(1)} \left[\psi_{;3} + \zeta_{,3}^{(1)} \right] \Big|_{y_3 = (\phi_1 - \frac{1}{2})h} \\ &= K_{13}^{(2)} \psi_{;1} + K_{23}^{(2)} \psi_{;2} + K_{33}^{(2)} \left[\psi_{;3} + \zeta_{,3}^{(2)} \right] \Big|_{y_3 = (\phi_1 - \frac{1}{2})h} \end{aligned} \quad (22)$$

Clearly this differential statement contains two second-order ordinary differential equations in Eq. (17) and five constraints to solve for $\zeta^{(\alpha)}$ and λ . The solution of λ is found to be zero and $\zeta^{(\alpha)}$ are linear functions of y_3 . Having solved the fluctuation functions, $\zeta^{(\alpha)}$, the [density of “energy” integral of this effective materials](#) can be [trivially](#) obtained as:

$$\Pi_\Omega = \frac{1}{2} \begin{Bmatrix} \psi_{;1} \\ \psi_{;2} \\ \psi_{;3} \end{Bmatrix}^T \begin{bmatrix} K_{11}^* & K_{12}^* & K_{13}^* \\ K_{12}^* & K_{22}^* & K_{23}^* \\ K_{13}^* & K_{23}^* & K_{33}^* \end{bmatrix} \begin{Bmatrix} \psi_{;1} \\ \psi_{;2} \\ \psi_{;3} \end{Bmatrix} \quad (23)$$

with the effective thermal conductivity coefficients K_{ij}^* as

$$K_{11}^* = \langle K_{11} \rangle - \frac{(K_{13}^{(1)} - K_{13}^{(2)})^2 \phi_1 \phi_2}{K_{33}^{(2)} \phi_1 + K_{33}^{(1)} \phi_2} \quad (24)$$

$$K_{22}^* = \langle K_{22} \rangle - \frac{(K_{23}^{(1)} - K_{23}^{(2)})^2 \phi_1 \phi_2}{K_{33}^{(2)} \phi_1 + K_{33}^{(1)} \phi_2} \quad (25)$$

$$K_{33}^* = \frac{K_{33}^{(1)} K_{33}^{(2)}}{\phi_2 K_{33}^{(1)} + \phi_1 K_{33}^{(2)}} \quad (26)$$

$$K_{12}^* = \langle K_{12} \rangle - \frac{(K_{13}^{(1)} - K_{13}^{(2)})(K_{23}^{(1)} - K_{23}^{(2)}) \phi_1 \phi_2}{\phi_2 K_{33}^{(1)} + \phi_1 K_{33}^{(2)}} \quad (27)$$

$$K_{13}^* = \frac{K_{13}^{(1)} K_{33}^{(2)} \phi_1 + K_{13}^{(2)} K_{33}^{(1)} \phi_2}{\phi_2 K_{33}^{(1)} + \phi_1 K_{33}^{(2)}} \quad (28)$$

$$K_{23}^* = \frac{K_{23}^{(1)} K_{33}^{(2)} \phi_1 + K_{23}^{(2)} K_{33}^{(1)} \phi_2}{\phi_2 K_{33}^{(1)} + \phi_1 K_{33}^{(2)}} \quad (29)$$

It is interesting to note that K_{33}^* is the same as the rule of mixtures based on Reuss’s hypothesis for this special case. If $K_{13}^{(1)} = K_{13}^{(2)}$ and $K_{23}^{(1)} = K_{23}^{(2)}$, then K_{11}^* , K_{22}^* , and K_{12}^* are the same as the [rule of mixtures](#) based on Voigt’s hypothesis, and K_{13}^* and K_{23}^* are the same as the constituent properties.

4 Finite Element Implementation

For more general cases, we need to rely on numerical solutions. Here, we will implement the variational statement in Eq. (13) using the well-established FEM. It is possible to formulate the FEM solution based on Eq. (13), however, it is not the most convenient and efficient way because Lagrange multipliers will increase the number of unknowns. To this end, we can reformulate the variational statement in Eq. (13) as the stationary value of the following functional

$$\Pi_{\Omega} = \frac{1}{2\Omega} \int_{\Omega} K_{ij} (\psi_{;i} + \zeta_{;i}) (\psi_{;j} + \zeta_{;j}) d\Omega \quad (30)$$

under the following three constraints

$$\zeta^{+i} = \zeta^{-i} \quad \text{for } i = 1, 2, 3 \quad (31)$$

The constraint in Eq. (12) does not affect the minimum value of Π_{Ω} but help uniquely determine ζ . In practice, we can constrain the fluctuation function at an arbitrary node to be zero and later use this constraint to recover the unique fluctuation function. It is fine to use penalty function method to introduce the constraints in Eqs. (31). However, this method introduces additional approximation and the robustness of the solution depends on the choice of large penalty numbers. Here, we choose to make the nodes on the positive boundary surface (*i.e.*, $y_i = d_i/2$) slave to the nodes on the opposite negative boundary surface (*i.e.*, $y_i = -d_i/2$). By assembling all the independent active degrees of freedom, we can implicitly and exactly incorporate the constraints in Eqs. (31). In this way, we also reduce the total number of unknowns in the linear system which will be formulated as follows.

Introduce the following matrix notations

$$\Phi = [\psi_{;1} \ \psi_{;2} \ \psi_{;3}]^T \quad (32)$$

$$\Phi_1 = \begin{Bmatrix} \frac{\partial \zeta}{\partial y_1} \\ \frac{\partial \zeta}{\partial y_2} \\ \frac{\partial \zeta}{\partial y_3} \end{Bmatrix} = \begin{Bmatrix} \frac{\partial}{\partial y_1} \\ \frac{\partial}{\partial y_2} \\ \frac{\partial}{\partial y_3} \end{Bmatrix} \zeta \equiv \Gamma_h \zeta \quad (33)$$

where Γ_h is an operator matrix. If we discretize ζ using the finite elements as

$$\zeta(x_i; y_i) = G(y_i) \xi(x_i) \quad (34)$$

where G representing the shape functions and ξ a column matrix of the nodal values of the fluctuation function. Substituting Eqs. (32), (33), and (34) into

Eq. (30), we obtain a discretized version of the functional as

$$\Pi_{\Omega} = \frac{1}{2\Omega} (\xi^T F \xi + 2\xi^T K_{h\Phi} \Phi + \Phi^T K_{\Phi\Phi} \Phi) \quad (35)$$

where

$$F = \int_{\Omega} (\Gamma_h G)^T K (\Gamma_h G) d\Omega \quad K_{h\Phi} = \int_{\Omega} (\Gamma_h G)^T K d\Omega \quad K_{\Phi\Phi} = \int_{\Omega} K d\Omega \quad (36)$$

with K as the 3×3 matrix of K_{ij} . Minimizing Π_{Ω} in Eq. (35), we obtain the following linear system

$$F \xi = -K_{h\Phi} \Phi \quad (37)$$

It is clear from Eq. (37) that the fluctuation function ξ is linearly proportional to Φ , which means the solution can be written symbolically as

$$\xi = \xi_0 \Phi \quad (38)$$

Substituting Eq. (38) into Eq. (35), we can calculate [the density of “energy” integral](#) of the UC as

$$\Pi_{\Omega} = \frac{1}{2\Omega} \Phi^T (\xi_0^T K_{h\Phi} + K_{\Phi\Phi}) \Phi \equiv \frac{1}{2} \Phi^T K^* \Phi \quad (39)$$

It can be seen that K^* in Eq. (39) is the effective thermal conductivity matrix and Φ global temperature gradient.

If the local fields within UC are of interest, we can recover those fields including local temperature and heat flux in terms of the macroscopic behavior including the global temperature ψ and the corresponding gradient $\psi_{;i}$, and the fluctuation function ζ . First, we need to uniquely determine the fluctuation function. Otherwise, we could not uniquely determine the local temperature field. [Because we have fixed an arbitrary node and made nodes on the positive boundary surfaces \(*i.e.*, \$y_i = +d_i/2\$ \) slave to the corresponding negative boundary surfaces \(*i.e.*, \$y_i = -d_i/2\$ \) in forming the linear system in Eq. \(37\), we need to construct a new array \$\xi_0\$ from \$\xi_0\$ by assigning the values for slave nodes according to the corresponding active nodes and assign zero to the fixed node. Clearly, \$\xi_0\$ corresponds to the stationary value of \$\Pi_{\Omega}\$ in Eq. \(30\) under \[constrains in Eqs. \\(31\\)\]\(#\). However, \$\xi_0\$ may not satisfy Eq. \(12\). The real solution, denoted as \$\bar{\xi}_0\$ can be found trivially by adding a constant to each node so that Eq. \(12\) is satisfied.](#)

After having determined the fluctuation functions uniquely, we can recover the local temperature using Eqs. (9) and (11) as

$$\phi = \psi + y_i \psi_{;i} + \bar{G} \bar{\xi}_0 \Phi \quad (40)$$

where \bar{G} is different from G due to the recovery of slave nodes and the constrained node. The local temperature gradient field can be recovered using

Eqs. (3) and (33) as

$$[\phi_{,1} \quad \phi_{,2} \quad \phi_{,3}]^T = \Phi + \Gamma_h \bar{G} \bar{\xi}_0 \Phi \quad (41)$$

Finally, the local heat flux field can be recovered straightforwardly using the 3D Fourier law for the constituent materials as

$$q_i = -K_{ij} \phi_{,j} \quad (42)$$

We have implemented this formulation in the computer program VAMUCH. In the next section, we will use a few numerical examples to demonstrate the application and accuracy of this theory and code.

5 Numerical Examples

VAMUCH provides a unified analysis for general 1D, 2D, or 3D UCs. First, the same code VAMUCH can be used to homogenize binary composites (modeled using 1D UCs), fiber reinforced composites (modeled using 2D UCs), and particle reinforced composites (modeled using 3D UCs). Second, VAMUCH can reproduce the results for lower-dimensional UCs using higher-dimensional UCs. That is, VAMUCH predicts the same results for binary composites using 1D, 2D or 3D UCs, and for fiber reinforced composites using 2D or 3D UCs.

In this section, several examples will be used to demonstrate the accuracy of VAMUCH for predicting the effective thermal conductivity and calculating the local heat flux field within UC due to temperature gradients. To facilitate comparison with existing models in the literature, we only consider composites with isotropic constituents although the present method and code can handle general anisotropic constituents.

5.1 *Effective thermal conductivity of fiber reinforced composites*

The first example is a carbon fiber reinforced aluminum matrix composite. Both constituents are isotropic with thermal conductivity $K = 129 \text{ W}/(\text{m} \cdot \text{K})$ for the carbon fiber, and $K = 237 \text{ W}/(\text{m} \cdot \text{K})$ for aluminum matrix. The fiber is of circular shape and arranged in a square array. The prediction of VAMUCH for the effective thermal conductivity along the fiber direction exactly obeys the rule of mixtures, which has been generally accepted as the exact solution for the longitudinal thermal conductivity for fiber reinforced composites with isotropic constituents (Hashin, 1968).

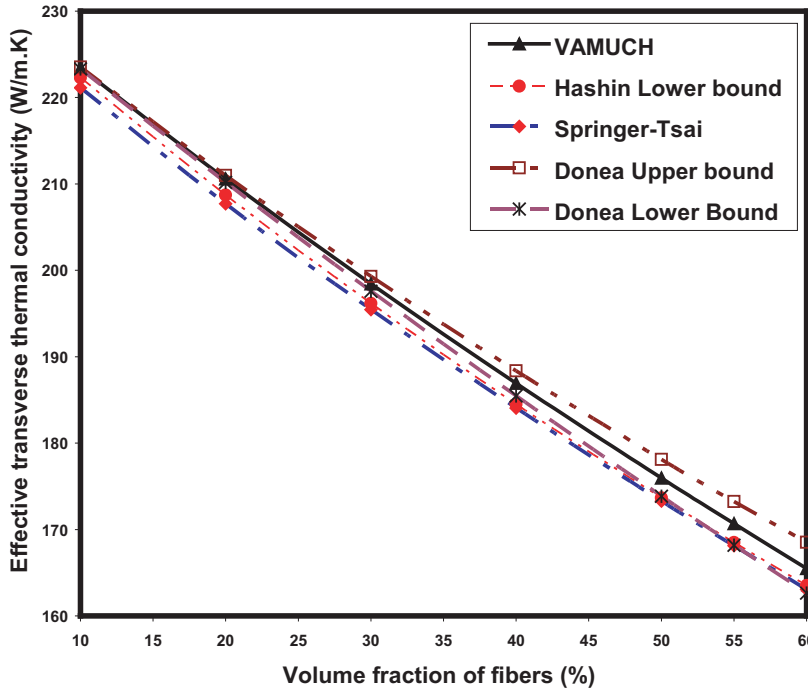


Fig. 3. Effective transverse thermal conductivity of the carbon/Al composite

However, the effective thermal conductivity coefficients in the transverse directions (K_{22}^* and K_{33}^*) do not in general obey the rule of mixtures. To validate the present theory, we compare VAMUCH prediction with other models in the literature (Donea, 1972; Behrens, 1968; Hatta and Taya, 1986; Hashin, 1983; Springer and Tsai, 1967). As shown in Fig. 3, VAMUCH results are perfectly located between the variational bounds of Donea (1972), while the Springer-Tsai model (Springer and Tsai, 1967) and the lower bound of Hashin (1983) underpredict the results. We have also found out that VAMUCH results are on the top of those obtained by Behrens (1968), Hatta and Taya (1986), and the upper bound of Hashin (1983) and these results are not shown in the plot for clarity.

The second example is a boron fiber reinforced aluminum composite with constituents as isotropic with thermal conductivity $K = 27.4 \text{ W}/(\text{m} \cdot \text{K})$ for the boron fiber, and $K = 237 \text{ W}/(\text{m} \cdot \text{K})$ for aluminum matrix. The fiber is still circular and arranged in a square array. The effective thermal conductivity computed by different models are plotted in Fig. 4. We found out that the results of Hashin upper bound (Hashin, 1983) are the same as those of Behrens (1968) and Hatta and Taya (1986). Hence only Hashin upper bound is plotted in the figure. It can be observed that the predictions of Hashin upper bound are slightly higher than those of VAMUCH when the fiber volume fraction is higher than 40%. We also observe that the difference between Hashin upper and lower bounds (Hashin, 1983) is significant for this case which means they are not very

useful for composites with constituents having relatively high contrast ratio in thermal conductivity properties. VAMUCH results are also nicely located in the much narrower bounds of Donea (1972), while the prediction of Springer and Tsai (1967) is not accurate for this case because it is even significantly lower than the lower bound of Donea (1972).

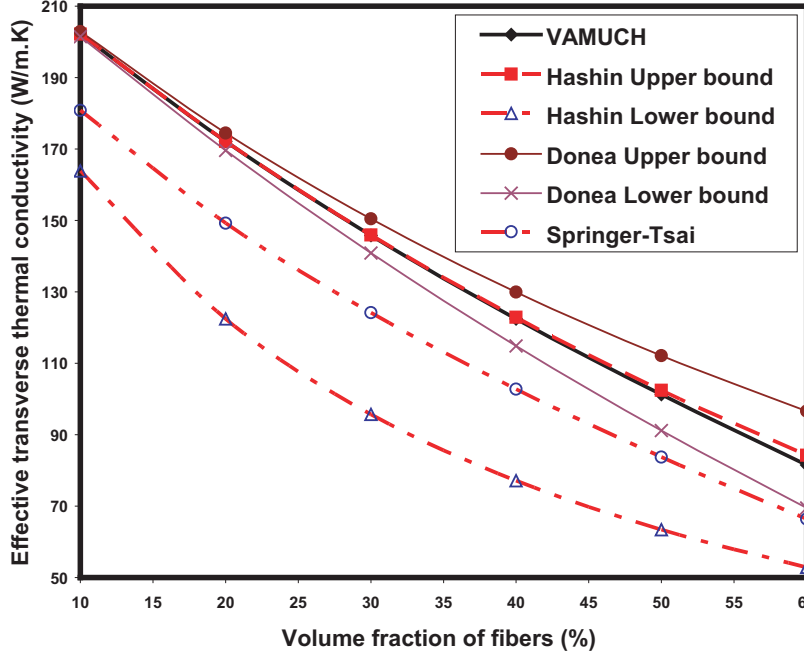


Fig. 4. Effective transverse thermal conductivity of the boron/Al composite

In the two examples we just studied, the thermal conductivity of matrix is higher than that of the fiber. Now, let us consider a glass/polypropylene composite with the thermal conductivity $K = 1.05 \text{ W}/(\text{m} \cdot \text{K})$ for the glass fiber, and $K = 0.2 \text{ W}/(\text{m} \cdot \text{K})$ for the polypropylene matrix. We plot the change of effective transverse thermal conductivity of composites with respect to volume fraction of fibers in Fig. 5. Again, we find out that VAMUCH results lie between the variational bounds of Donea (1972). And the results of Hashin lower bound (Hashin, 1983), Behrens (1968), and Hatta and Taya (1986) are identical but slightly lower than VAMUCH results when the volume fraction of fibers is higher than 40%. Similarly, as in the previous case, we can observe that Donea (1972) provides much narrower bounds than Hashin (1983) for this case.

We also use ANSYS, a commercial FEM package, to calculate the effective thermal conductivities of these three fiber reinforced composites. According to Islam and Pramila (1999), we apply isothermal conditions to the edges perpendicular to the direction we want to evaluate the thermal conductivity and apply adiabatic conditions to the edges parallel to this direction. The

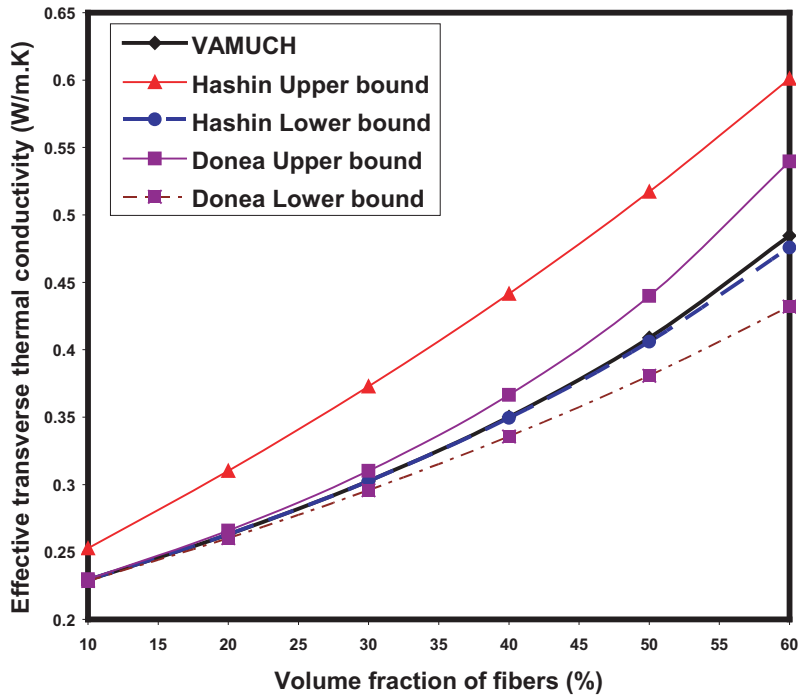


Fig. 5. Effective transverse thermal conductivity of the glass/polypropylene composite

effective thermal conductivity is obtained by the ratio between the average heat flux and average temperature gradient. We found out that VAMUCH results are almost the same as the ANSYS results for similar discretization schemes.

To verify whether VAMUCH can deal with composites with very high contrast ratio and high volume fraction, we choose a composite formed by circular fibers arranged in square array. The volume fraction of fibers is 65%. We fix the thermal conductivity of matrix at $1 \text{ W}/(\text{m} \cdot \text{K})$, while the thermal conductivity of the fiber varies from 10 to 10^4 . We plot the effective thermal conductivity computed using different approaches at different contrast ratio in Fig. 6. It can be seen that VAMUCH results are on the top of ANSYS results and lie between Donea variational bounds. And the results of Hashin lower bound (Hashin, 1983) are identical to those obtained from Behrens (1968), Halpin-Tsai (Progelfhof et al., 1976), and Hatta and Taya (1986). It is obvious that these approaches underpredict the results. At different contrast ratio, the Hashin upper bounds are too large to be nicely plotted in the same figure.

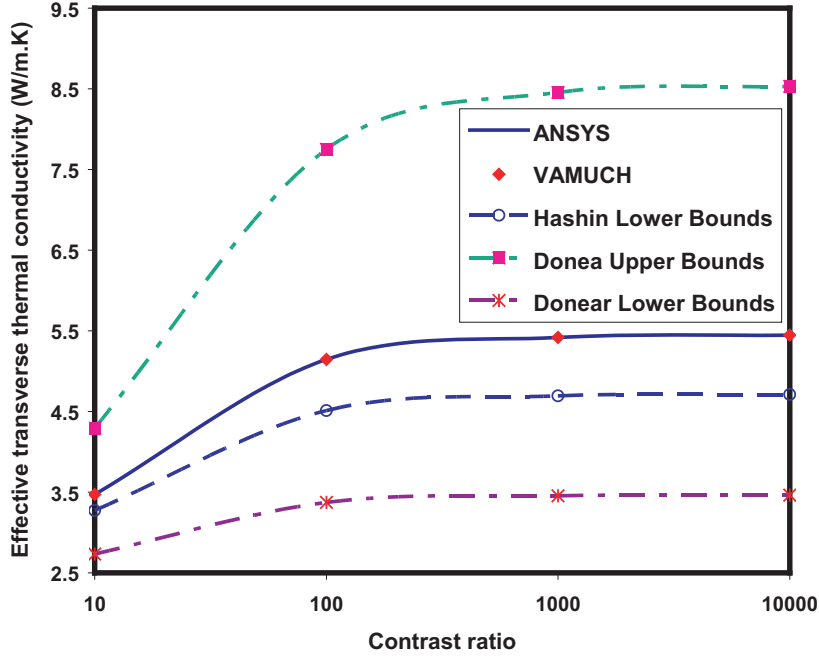


Fig. 6. Effective transverse thermal conductivity with respect to varying contrast ratios

5.2 Effective thermal conductivity of particle reinforced composites

Due to special arrangements of constituents of particle reinforced composites, 3D UCs are required to accurately model the microstructures. In this section, we will use VAMUCH to analyze two typical particle reinforced composites to validate the 3D predictive capability of VAMUCH.

The first example is a SiC particle reinforced aluminum composite. The spherical SiC particles are embedded in a triply periodic cubic array. Both constituents are isotropic with thermal conductivity $K = 120 \text{ W}/(\text{m} \cdot \text{K})$ for SiC particles, and $K = 237 \text{ W}/(\text{m} \cdot \text{K})$ for aluminum matrix. The change of effective thermal conductivity of composites with respect to volume fraction of particles are plotted in Fig. 7. VAMUCH results have an excellent agreement with Hashin upper bound (Hashin, 1983), Budiansky (1970) and Cheng and Vachon (1970), although Budiansky (1970) and Cheng and Vachon (1970) slightly underpredict the results when the volume fraction of particles are higher than 20%. It was also found out that VAMUCH results are on the top of those calculated by McPhedran and McKenzie (1978). All these predictions are perfectly located between the variational bounds of Donea (1972). It can be obviously observed that the results of Lewis and Nielsen (2003) significantly underpredict the effective thermal conductivity in comparison to other approaches.

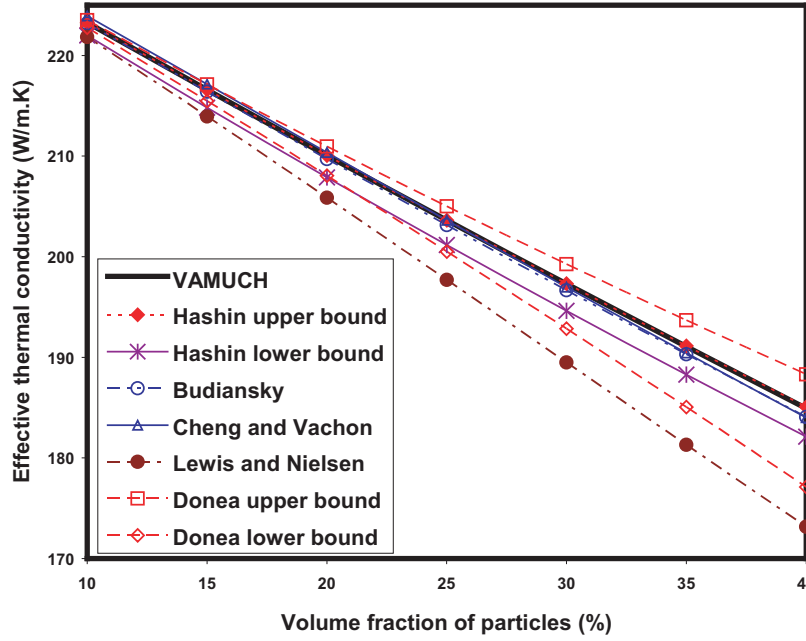


Fig. 7. Effective thermal conductivity of the Sic/Al composite

Another example is an alumina (Al_2O_3) particle reinforced polyethylene composite. This composite has the same microstructure as the previous example. Both components are also isotropic with thermal conductivity $K = 31 \text{ W}/(\text{m} \cdot \text{K})$ for alumina particles, and $K = 0.545 \text{ W}/(\text{m} \cdot \text{K})$ for the polyethylene matrix. The contrast ratio of thermal conductivity of two components is as high as 56.88. The predictions of different approaches are shown in Fig. 8. VAMUCH results agree with [McPhedran and McKenzie \(1978\)](#) at different volume fraction and with the lower bound of Hashin (1983) very well if the volume fraction of particles is smaller than 25%. The prediction of Lewis and Nielsen (2003) is also very close to that of VAMUCH if the volume fraction of particles is very small. The difference between the variational bounds of Donea (1972) becomes too large to be useful for high volume fraction of particles. The prediction of Cheng and Vachon (1970) for this case cannot be considered as accurate because it is even not located between and lower and upper bounds of Donea (1972). We also need to point out that for this case, the results of Hashin upper bound are too different from the lower bound and cannot nicely plotted in the same figure.

We also analyzed these two examples of particle reinforced composites using ANSYS following the approach of Kumlutas and Tavman (2006). Again, we found out VAMUCH results are identical to ANSYS results if similar meshes are used for both approaches.

It is noted that Hashin bounds are known to be the best possible bounds for statistically isotropic or transversely isotropic composites, when the only avail-

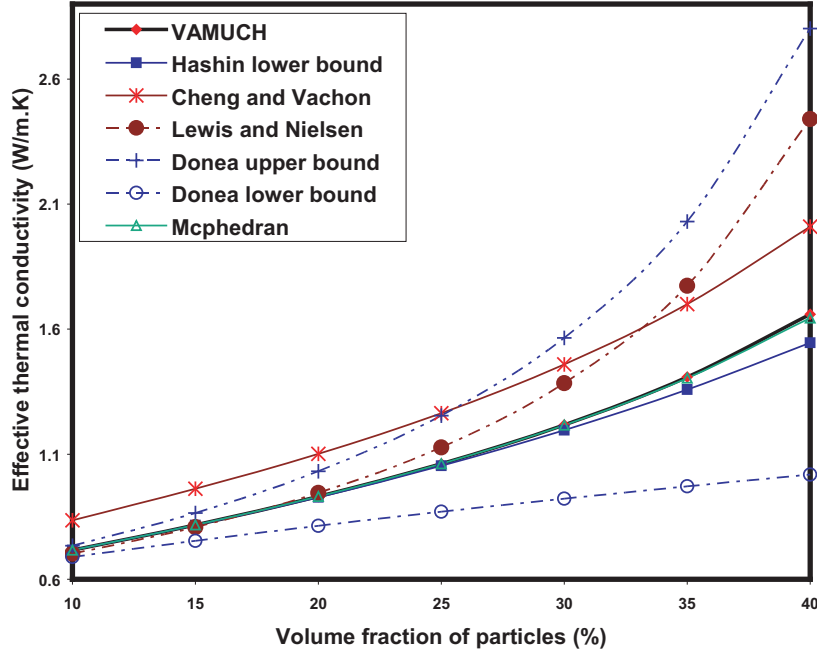


Fig. 8. Effective thermal conductivity of the Al_2O_3 /polyethylene composite

able geometrical information is the phase volume fractions (Hashin and Shtrikman, 1962). However, such bounds can be improved if additional information such as shape of inclusions, geometry of microstructure added into the formulation (Hashin, 1983). It has been shown that Hashin lower bound or upper bound is the exact solution for composite spheres assemblage (CSA) (Hashin, 1968), which explains why one of Hashin bounds agrees with VAMUCH very well if the inclusion volume fraction is not very large. Donea bounds (Donea, 1972) are not rigorous variational bounds. Rather the material is considered as a composition of CSA within the largest possible circle/sphere and matrix. The Voigt rule of mixtures is used to obtain the Donea upper bound and the Ruess rule of mixtures is used to obtain the Donea lower bound. The effective properties of CSA use those of Hashin (1968), which is also one of the Hashin bounds. Therefore, Donea bounds will fall outside at least one of Hashin bounds, as consistently shown in these examples. The gap between Donea bounds could be smaller than that of Hashin bounds because more information has been used in obtaining Donea bounds.

5.3 Recovery of local heat flux

VAMUCH can accurately recover the local heat flux distribution within the UC due to temperature gradients. We will use ANSYS results as benchmark to verify the prediction of VAMUCH. Firstly, we consider the glass/polypropylene fiber reinforced composite with fiber volume fraction as 0.2. Due to the differ-

ence of thermal conductivity of two components, the local heat flux distribution resulting from 100 K/m in the y_2 direction is not uniform within UC. The distribution contours of q_2 and q_3 are plotted in Figs. 9 and 10, respectively. The sudden changes of local heat flux around the interface between the fibers and the matrix are well captured by VAMUCH. For quantitative comparison, we also plot the local heat flux distribution q_2 along $y_2 = 0$ predicted by VAMUCH and ANSYS in Fig. 11. It can be seen that there are an excellent match between these two sets of results.

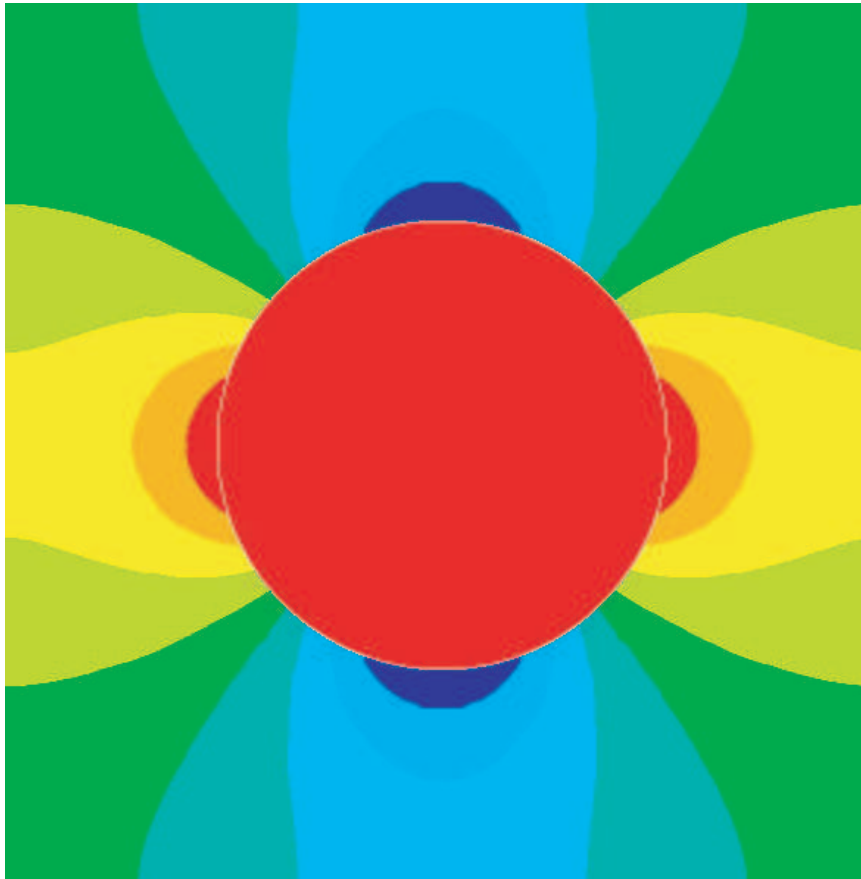


Fig. 9. Contour plot of heat flux q_2 in the glass/polypropylene composite

Secondly, we choose a special example which is a composite having an X-shape microstructure. The local heat flux distribution predicted by VAMUCH is shown in Fig. 12. There are narrow necks at corner contacts between the reinforcements which exhibit significant fluctuation of the local heat flux. The local heat flux distributions along the diagonal line predicted by VAMUCH and ANSYS are plotted in Fig. 13. Excellent match between these two approaches is clear from this plot.

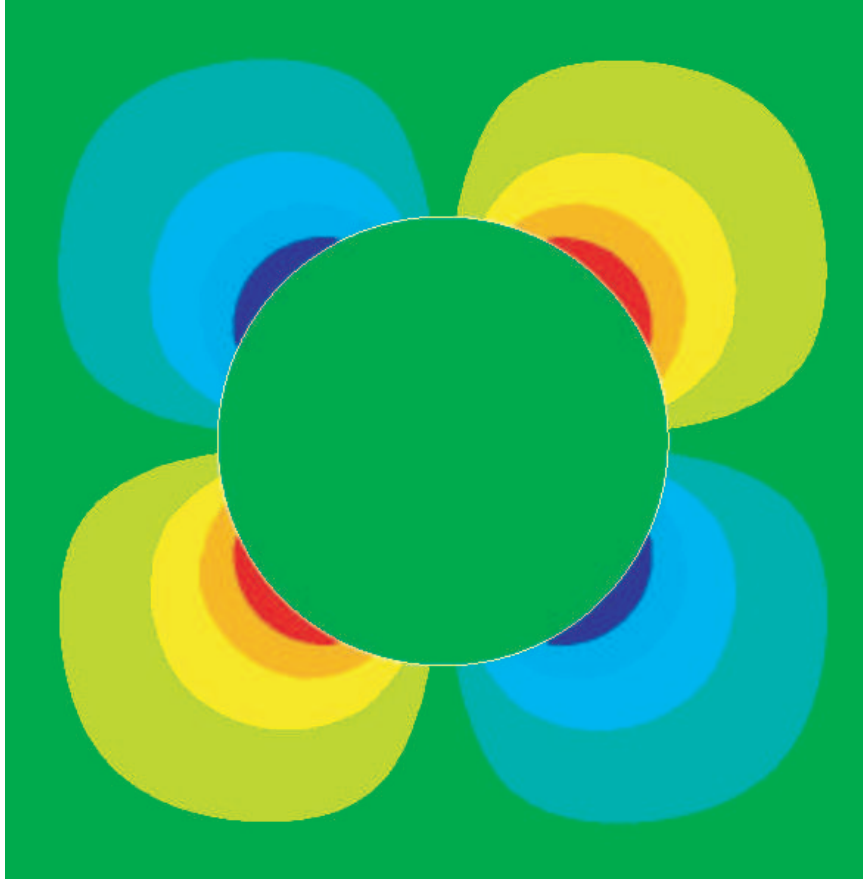


Fig. 10. Contour plot of heat flux q_3 in the glass/polypropylene composite

6 Conclusion

The variational asymptotic method for unit cell homogenization (VAMUCH) has been extended to predict effective thermal conductivity coefficients of composites. In comparison to existing models, the present theory has the following unique features:

- (1) It adopts the variational asymptotic method as its mathematical foundation. It invokes only essential assumptions inherent in the concept of micromechanics.
- (2) It has an inherent variational nature and its numerical implementation is shown to be straightforward.
- (3) It handles 1D/2D/3D unit cells uniformly. The dimensionality of the problem is determined by that of the periodicity of the unit cell.

The present theory is implemented in the computer program, VAMUCH. Numerous examples have clearly demonstrated its application and accuracy as a general-purpose micromechanical analysis tool. Although for the examples we have studied, VAMUCH results are almost identical to ANSYS results,

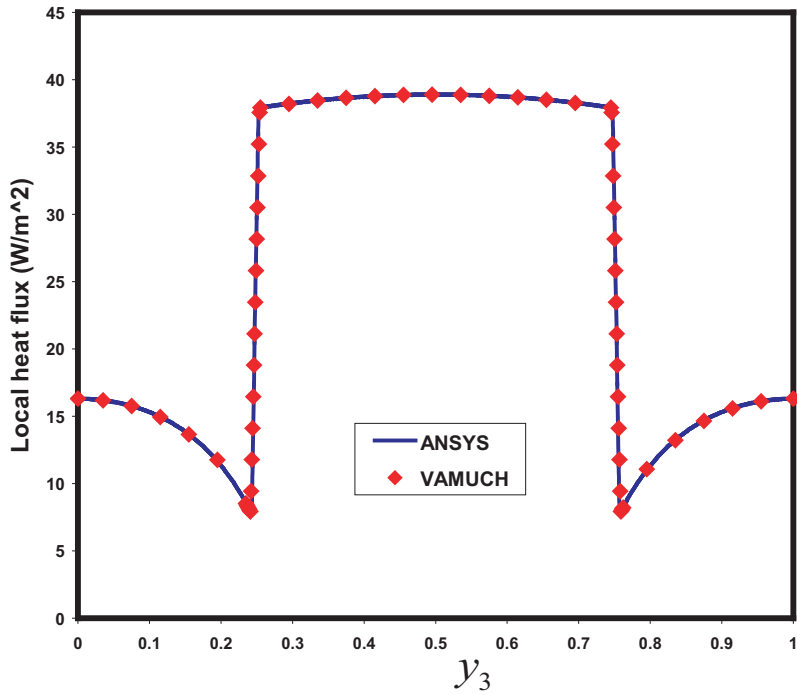


Fig. 11. Heat flux q_2 distribution along $y_2 = 0$ in the glass/polypropylene composite

VAMUCH has the following advantages over ANSYS for micromechanical analysis:

- (1) VAMUCH can obtain different material properties in different directions simultaneously, which is more efficient than those approaches requiring multiple runs under different temperature conditions.
- (2) VAMUCH can model general anisotropic heterogeneous materials with constituents having full anisotropy (with six material constants for thermal conductivity), while ANSYS and other FEM package can only handle constituents up to orthotropic (with three material constants for thermal conductivity). The current FEM approaches for predicting thermal conductivity (Islam and Pramila, 1999; Kumlutas and Tavman, 2006) are restricted to be at most macroscopically orthotropic, which is an unnecessary restriction.
- (3) VAMUCH calculates effective properties and local fields directly with the same accuracy as the fluctuation functions. No postprocessing calculations which introduces more approximations, such as averaging temperature gradient and heat flux, are needed.

As a byproduct of validating VAMUCH, we also provided a brief assessment of existing models for predicting effective thermal conductivity.

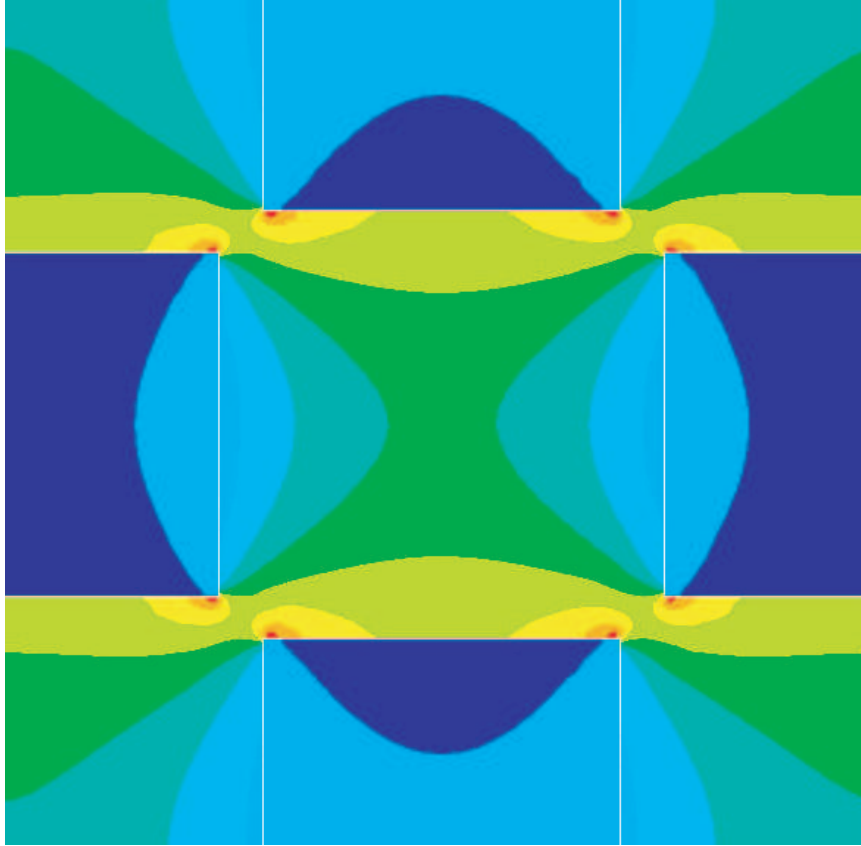


Fig. 12. Contour plot of heat flux of an X-shape composite

Due to the mathematical analogy of heat conduction, electrostatics, magnetostatics, and diffusion, the present theory and the companion code can also be used to predict effective [dielectric](#), [magnetic](#), and diffusion properties of heterogeneous materials.

7 Acknowledgements

This study is supported by the National Science Foundation under Grant DMI-0522908. The views and findings contained herein are those of the authors and should not be interpreted as necessarily representing the official policies or endorsement, either expressed or implied, of the National Science Foundation.

References

Behrens, E., 1968. Thermal conductivities of composite materials. *Journal of Composite Materials* 2, 2–17.

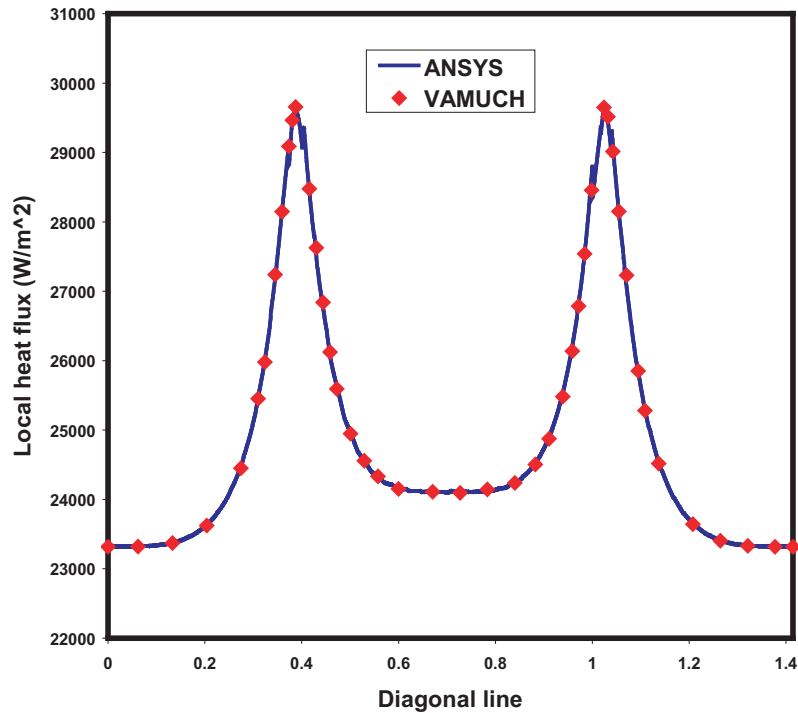


Fig. 13. Heat flux of of the X-shape composite along the diagonal line

- Berdichevsky, V. L., 1977. On averaging of periodic systems. *PMM* 41 (6), 993 – 1006.
- Budiansky, B., 1970. Thermal and thermoelastic properties of isotropic composites. *Journal of Composite Materials* 4, 286–295.
- Cheng, S., Vachon, R., 1970. A technique for predicting the thermal conductivity of suspensions, emulsions and porous materials. *International Journal of Heat and Mass Transfer* 13, 537–546.
- Donea, J., 1972. Thermal conductivities based on variational principles. *Journal of Composite Materials* 6, 262–266.
- Ganapathy, D., Singh, K., Phelan, P., Prasher, R., 2005. An effective unit cell approach to compute the thermal conductivity of composites with cylindrical particles. *Journal of Heat Transfer* 127, 553–559.
- Hashin, Z., 1968. Assessment of the self consistent scheme approximation: conductivity of particulate composites. *Journal of Composite Materials* 2, 284–300.
- Hashin, Z., 1983. Analysis of composite materials-a survey. *Applied Mechanics Review* 50, 481–505.
- Hashin, Z., Shtrikman, S., 1962. A variational approach to the theory of the effective magnetic permeability of multiphase materials. *Journal of Applied Physics* 33, 3125–3131.
- Hatta, H., Taya, M., 1986. Thermal conductivity of coated filler composites. *Journal of Applied Physics* 59, 1851–1860.
- Islam, M. R., Pramila, A., 1999. Thermal conductivity of fiber reinforced com-

- posites by the FEM. *Journal of Composite Materials* 33, 1699–1715.
- Kumlutas, D., Tavman, I., 2006. A numerical and experimental study on thermal conductivity of particle filled polymer composites. *Journal of Thermoplastic Composite Materials* 19, 441–455.
- Kunin, I., 1982. *Theory of Elastic Media with Microstructure*. Vol. 1 and 2. Springer Verlag.
- Lee, Y.-M., Yang, R.-B., Gau, S.-S., 2006. A generalized self consistent method for calculation of effective thermal conductivity of composites with interfacial contact conductance. *International Communications in Heat and Mass Transfer* 33, 142–150.
- Lewis, T., Nielsen, L., 2003. Dynamic mechanical properties of particulate-filled composites. *Journal of Applied Polymer Science* 14, 1449–1471.
- McPhedran, R. C., McKenzie, D. R., 1978. The conductivity of lattices of spheres I. the simple cubic lattice. *Proc. R. Soc. Lond. A* 359, 45–63.
- Progelhof, R., Throne, J., Ruetsch, R., 1976. Methods for predicting the thermal conductivity of composite systems: a review. *Polymer Engineering and Science* 16, 615–625.
- Ramani, K., Vaidyanathan, A., 1995. Finite element analysis of effective thermal conductivity of filled polymeric composites. *Journal of Composite Materials* 29, 1725–1740.
- Springer, G., Tsai, S., 1967. Thermal conductivities of unidirectional materials. *Journal of Composite Materials* 1, 167–173.
- Xu, Y., Yagi, K., 2004. Calculation of the thermal conductivity of randomly dispersed composites using a finite element modeling method. *Materials Transactions* 45, 2602–2605.
- Yu, W., Tang, T., 2007a. Variational asymptotic method for unit cell homogenization of periodically heterogeneous materials. *International Journal of Solids and Structures* 44, 3738–3755.
- Yu, W., Tang, T., 2007b. A variational asymptotic micromechanics model for predicting thermoelastic properties of heterogeneous materials. *International Journal of Solids and Structures*, to appear.